INTERNATIONAL CONFERENCE ON LIGHTNING PROTECTION
33rd International Conference on Lightning Protection
25 - 30 September 2016
Estoril, Portugal

Measured Results of Gronding Electrode Impedances - Effect of Electrode Shape -

Akihiro Ametani
École Polytechnique de Montréal
Monteal, Canada

Koichi Yamabuki
National Institute of Technology,
Wakayama College
Wakayama, Japan

Hiroshi Morii and Takashi Kubo
Kansai Electric Power Company
Osaka, Japan

Abstract— **This paper investigates grounding impedance reduction with various shapes of grounding electrodes in comparison with a conventional vertical rod based on field tests. It is found that a vertical rectangular conducting plate is effective to reduce the transient and steady-state impedance less than a half of that of the vertical rod. A circular conducting plate parallel to the earth surface is also effective to reduce the steady-state impedance, but the transient impedance is nearly the same as that of the vertical rod. The rate of the reduction is somehow proportional to the surface area of the electrode, but tends to saturate as the area increases. It is confirmed that an FDTD gives a reasonable accuracy compared with the measured results.**

Keywords- field test, vertical electrode, plate electrode, grounding impedance, transient response, FDTD simulation

I. INTRODUCTION

There are a number of publications which discuss reduction of grounding impedances. Recently, many digital circuits are installed not only in power system control equipment but also in buildings and in home appliances. Thus, it becomes more important to reduce the grounding impedances to guarantee reliable operation of the digital circuits for both steady and transient states [1-4]. From the above, Kansai Electric Power Company (KEPCO) carried out a series of field tests to measure the grounding impedances.

A measured result involves noises due to mutual coupling between a current lead wire and a voltage reference wire, and also unknown parameters such as an earth resistivity and permittivity. On the contrary, a numerical electromagnetic analysis (NEA) method [5] can simulate a transient only by the geometrical and physical parameters of a given system, and thus the NEA method is very effective to analyze the transient responses of a grounding electrode buried in an earth of which the resistivity and the permittivity are not clear.

This paper shows field test results of transient and steady state responses on grounding electrodes with various shapes, i. e. a vertical rod, a rectangular plate, a circular plate etc. The field tests were carried out in different seasons for three years to obtain reliable results in Kansai Electric Power Co. The effect of electrode shapes on the reduction of grounding impedances are investigated based on the test results. Also, NEA simulations are carried out by using Visual Test Lab (VSTL) [6] which is based on a finite-difference time-domain (FDTD) method. A comparison with the measured results are made to confirm the accuracy of the VSTL.

II. FIELD MEASUREMENTS

A. Experimental setup

Field measurements were carried out in a test yard of the KEPCO located on a mountain foot for three times in different year and seasons. The earth resistivity of the test yard varies from 80 Ωm to 200 Ωm. Fig. 1 illustrates an experimental setup. A pulse generator (PG1, 2.6 kV/rise time 50 ns) and a noise simulator (PG2, 1.9 kV/ rise time less than 1 μs) were used as a voltage source, and were terminated by a matching resistance of 470 Ω to a grounding electrode for the PG. The PG was connected to a test electrode through a resistance of 2

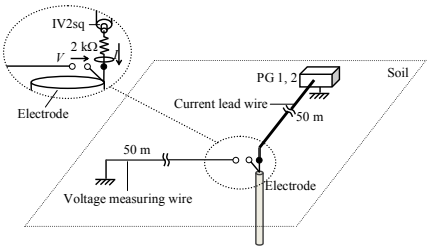

(a) Overview

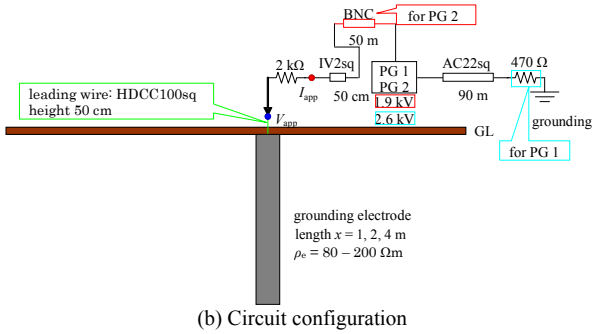

(b) Circuit configuration

Figure 1. Circuit configuration of experiments.

TABLE I. SPECIFICATIONS OF VOLTAGE SOURCES AND MEASURING INSTRUMENTS

Measuring Equipment	Specifications
Voltage Source	【Pulse Generator: PG1】 Manufacturer: Cosmotec Maximum Output Voltage: 5 kV Waveform : 0.05/100 μs Power Capacity : 50 VA 【Noise Simulator: PG2】 Manufacturer: NoiseKen Model: INS-4040 Maximum Output Voltage: 4 kV Pulse Rise Time: < 1 ns Maximum Pulse Width: 1μs
Oscilloscope	Manufacturer: Tektronix Model: TPS2024 Isolated Channels: 4 ch Sample Rate: 2 GS/s Bandwidth: DC ~ 200 MHz
Voltage Probe	Manufacturer: Yokogawa Electric Model: 701944 Turns Ratio: 100: 1 Bandwidth: DC ~ 400 MHz Maximum Input Voltage: 1000 Vrms, 6000 Vpeak
CT (1)	Manufacturer: Pearson Model: 2100 Output: 1V/1A Rise Time : < 20 ns Maximum Peak Current : 500 A Option: BNC Cable(50 Ω), Feed-through Terminal(50 Ω)
CT (2)	Manufacturer: Pearson Model: 2877 Output: 1V/1A Rise Time : < 2 ns Maximum Peak Current : 100 A Option: BNC Cable(50 Ω), Feed-through Terminal(50 Ω)

kΩ to represent a lightning current. An applied current was measured by a surge current transformer (CT), and an electrode voltage was measured by a voltage probe. The specifications of the PGs, the CTs and the probe are given in Table 1. A current lead wire (IV2sq 50 m + AC22sq 90 m), a voltage reference wire (IV2sq 150 m) and the test electrode were set to be perpendicular to each other. The shapes of test electrodes are illustrated in Fig. 2.

B. Measured resutlss

Table 2 shows the shapes of tested electrodes and corresponding measured results of peak voltages and converged voltages at the end of the measurement (PG1 : t = 4.5 μs, PG2 : t = 450 ns) normalized by the peak current. Fig. 3 and 4 show measured current and voltage waveforms in the cases of PG1 ($T_f \approx 0.5$ μs) and PG2 ($T_f \approx 10$ μs) respectively. It is observed in Fig. 3 that the grounding impedance is mostly resistive. In Fig. 4, it shows a capacitive characteristic. In fact, the steady state resistance R_g measured separately is greater than the converged value at t = 450 ns as observed in Table 2 (b).

It is clear that the peak and the converged (called "steady-state" hereafter) values of the grounding resistance are significantly reduced in the rectangular plate case (Cases 2 and 3 in Fig. 2). For example, the peak and the steady-state resistances of Cases 2-1 and 3-1 (x = 1 m) are reduced to 1/2 to 1/3 of those of the rod case, Case1-1. The steady-state resistance of Case 6 is a half of that of Case4-3 (pipe electrode) as observed in Table 2 (b) and Fig. 4. However, the circular plate of Case 7 shows no reduction of the grounding resistance. It is reasonable that the grounding resistance becomes smaller as the electrode length becomes longer. For Cases 1 and 4 in Table 2, the steady-state resistance evaluated by Sunde's formula [7] is given as reference. For the evaluation of the resistance for the L-type rod in Case 1, it is represented by an equivalent circular cylinder with the radius of r_e which gives the same surface area as that of the L-type rod. This equivalence has been confirmed to be reasonable from a comparison of the measured and simulation results. It looks an interesting subject to develop a theoretical formula of the grounding impedance for the electrodes of Cases 2 to 7 in Fig. 2.

Any measured result of a grounding impedance involves unknown physical parameters, such as earth resistivities along the earth surface and buried depth, not identical waveforms of an applied current in each case and a noise during a measurement. Thus it is not straightforward to discuss a difference between measured results. For the uncertainty, simulations by a numerical electromagnetic analysis method might be very effective [5].

III. FDTD SIMULATIONS

A. Simulation model

Fig. 5 illustrates an example of a model circuit for an FDTD simulation by using VSTL [6]. For x = 1 m, the analytical space is taken to be x_1 = 1.82 m. $x_2 = z = y$ = 1.42 m with the cell size of Δs = 0.01 m. The boundaries of the space is represented by Liao's second order absorbing boundary [5]. The electrode is assumed to be perfectly conducting. The voltage of the electrode at the sending end is calculated by integrating the electric field from the absorbing boundary.

B. Comparison with measured results

Fig. 6 and Fig. 7 show FDTD simulation results corresponding to measured results in Fig. 3 and Fig. 4. Also, the simulation results of peak and steady-state voltages are given in Table 2. In the simulation, the earth resistivity is set to be 150 Ωm and the relative permittivity 10. It is observed in the table and figures that the simulation results agree reasonably well with the measured results. Thus, it is quite possible to investigate the effect of electrode shapes on the reduction of grounding impedances based on simulation results by NEA methods.

IV. CONCLUSIONS

Field test results of transient responses on various grounding electrodes have been described, and the effect of electrode shapes on the grounding impedance reduction is investigated. Summarizing the investigations in the paper, the following concluding remarks are obtained.

(1) A vertical rectangular plate can reduce a grounding impedance in transient and steady states less than a half in comparison with that of a conventional vertical rod.

(2) A circular plate parallel to the earth surface is also effective to reduce a steady state resistance, but a transient impedance is nearly the same as that a vertical rod.

(3) The rate of impedance reduction is somehow proportional to the area of the electrode, but it tends to saturate as the area increases.

(4) It is confirmed that FDTD simulations give a reasonable agreement with the test results, and thus the FDTD can be used to study the transient characteristics of grounding electrodes.

REFERENCES

[1] Working Group (Chair: Agematsu, S.), Japanese Electrotechnical Research Association. Technologies of countermeasures against surges on protection relays and control systems. ETRA Report 57(3), 2002. (in Japanese).

[2] CIGRE WG C4-208, EMC within Power Plants and Substations. CIGRE-TB 543, 2013.

[3] IEC, Electromagnetic Compatibility Part 6-5 Generic Std. Immunity for power station and substation environments. IEC TC 61000-6-5, 2001.

[4] Japanese Electotechnical. Committee, Standard of Test Voltages for Low-Voltage Control Circuits in Power Stations and Substations. JEC-0103-2005, Tokyo: IEE Japan, 2005. (in Japanese).

[5] CIGRE WG C4-501(Convener: Ametani, A.), Guideline for Numerical Electromagnetic Analysis Method and its Application to Surge Phenomena. CIGRE-TB 543, 2013.

[6] CRIEPI, "Visual Surge Test Lab. (VSTL)", 2007, http://criepi.or.jp

[7] E. D. Sunde. Earth Conduction Effects in Transmission Systems. New York: Dover, 1968.

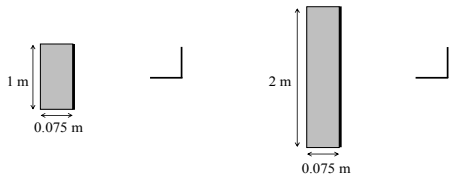

(a) L-type rod :Case 1

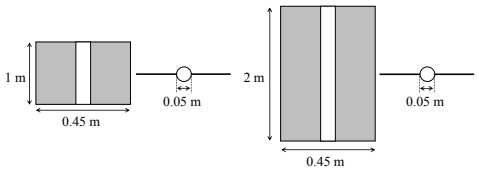

(b) Rectangular plate (width 0.45 m): Case 2

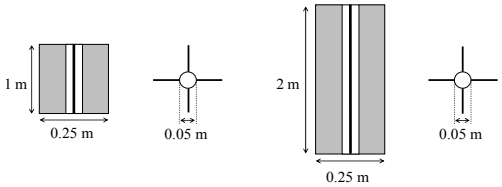

(c) Rectangular plate (width 0.25 m): Case 3

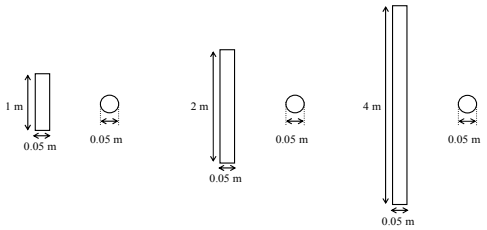

(d) Vertical pipe (radius 0.025 m): Case 4

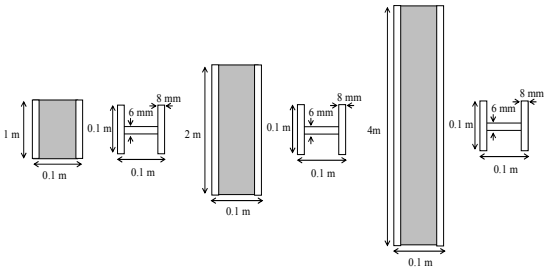

(e) H-type rod: Case 5

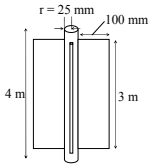

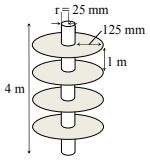

(f) 4 plates (fin type): Case 6 (g) 4 circular plates: Case 7

Figure 2. Electrode shapes

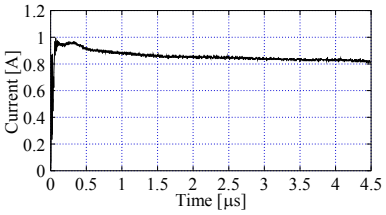

(a) Injected current

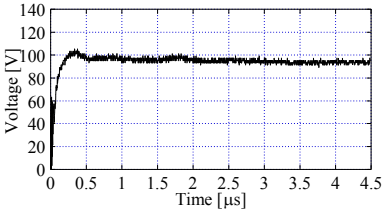

(b) Case 1-1: L-type rod, x = 1 m

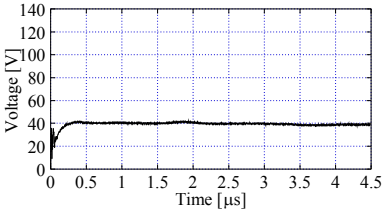

(c) Case 1-2: L-type rod, x = 2 m

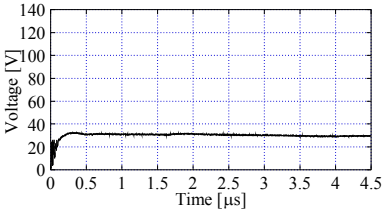

(d) Case 2-1: Plate (w 0.45 m), x = 1 m

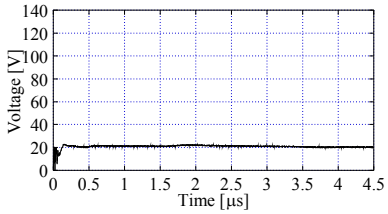

(e) Case 2-2: Plate (w 0.45 m), x = 2 m

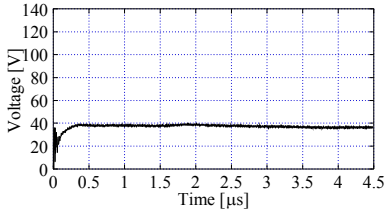

(f) Case 3-1: Plate (w 0.25 m), x = 1 m

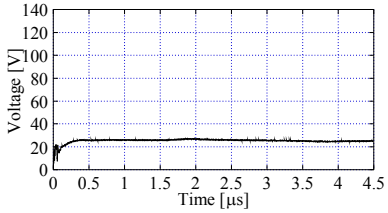

(g) Case 3-2: Plate (w 0.25 m), x = 2 m

Figure 3. Measured results of electrode transient voltages with a pulse generator: Cases 1 ~ 3

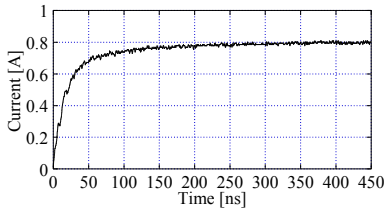

(a) Injected current

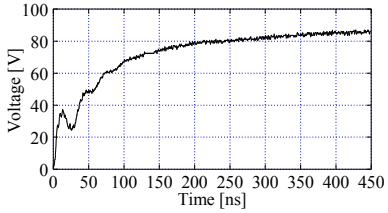

(b) Case 4-1:Pipe, x = 1 m

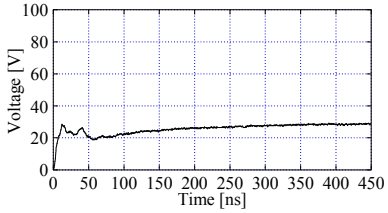

(c) Case 4-2: Pipe, x = 2 m

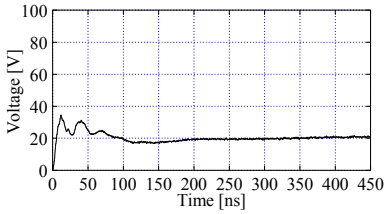

(d) Case 4-3: Pipe, x = 4 m

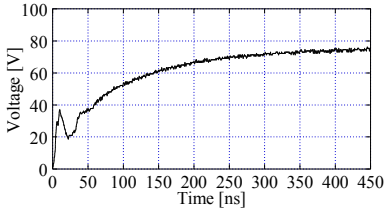

(e) Case 5-1: H-type rod, x = 1 m

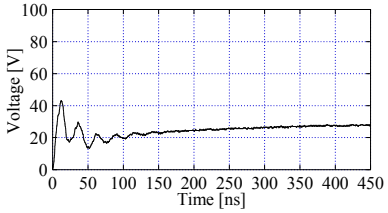

(f) Case 5-2: H-type rod, x = 2 m

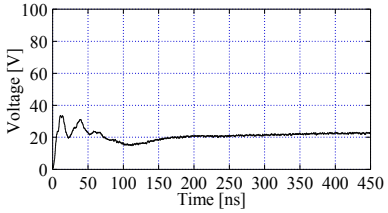

(g) Case 5-3: H-type rod, x = 4 m

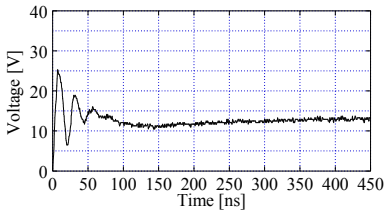

(h) Case 6: 4 plates (fin-type)

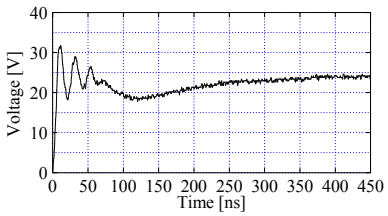

(i) Case 7: 4 circular plates

Figure 4. Measured results of electrode transient voltages with a noise simulator: Cases 4 – 7

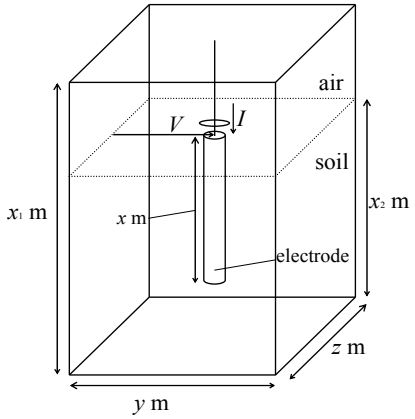

Figure 5. A model circuit for an FDTD simulation

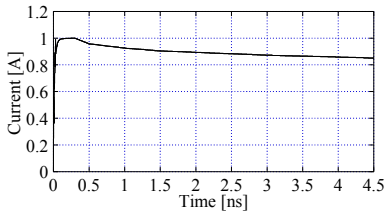

(a) Injected current

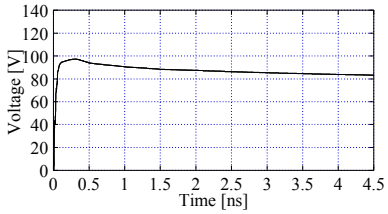

(b) Case 1-1: L-type rod, x = 1 m

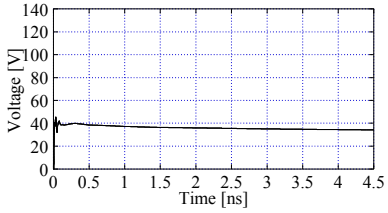

(c) Case 1-2: L-type rod, x = 2 m

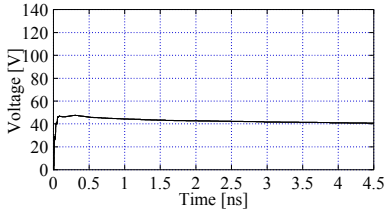

(d) Case 2-1:Plate (w 0.45 m), x = 1 m

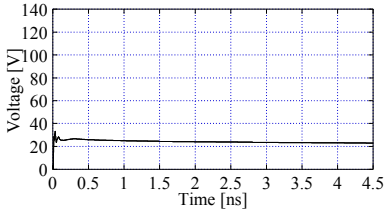

(e) Case 2-2: Plate (w 0.45 m), x = 2 m

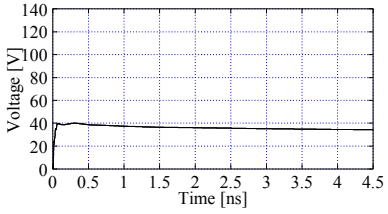

(f) Case 3-1: Plate (w 0.25 m), x = 1 m

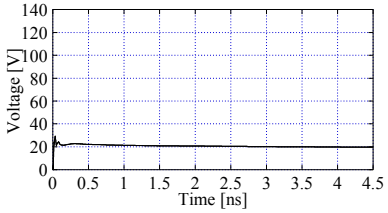

(g) Case 3-2: Plate (w 0.25 m), x = 2 m

Figure 6. FDTD simulation results corresponding to Fig. 3

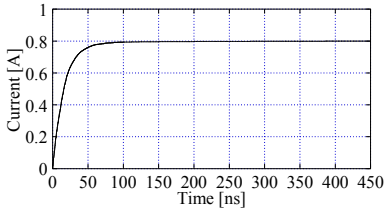

(a) Injected current

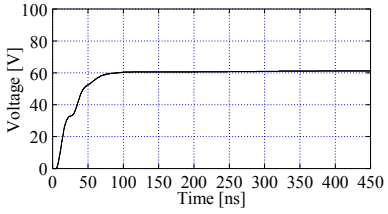

(b) Case 4-1:Pipe, x = 1 m

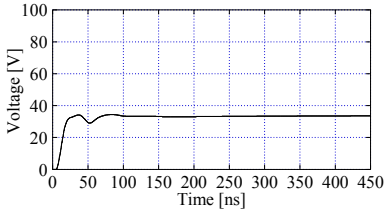

(c) Case 4-2: Pipe, x = 2 m

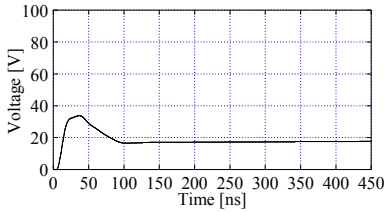

(d) Case 4-3: Pipe, x = 4 m

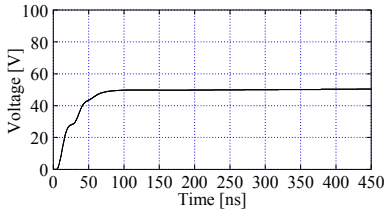

(e) Case 5-1: H-type rod, x = 1 m

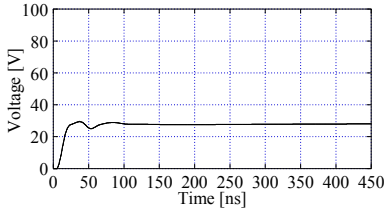

(f) Case 5-2: H-type rod, x = 2 m

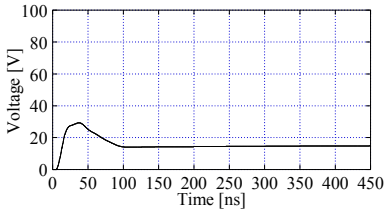

(g) Case 5-3: H-type rod, x = 4 m

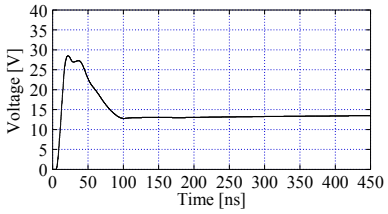

(h) Case 6: 4 plates (fin-type)

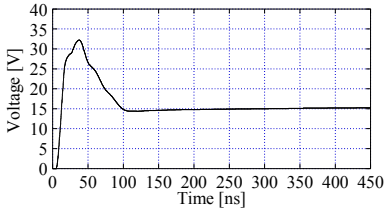

(i) Case 7: 4 circular plates

Figure 7. FDTD simulation results corresponding to Fig. 4

TABLE II. TRANSIENT PEAK VOLTAGES AND CONVERGED VALUES

(a) PG 1 - converged value at t = 4.5 μs

case	electrode shape	length x [m]	measured voltage [V/A]		simulation [V/A]		Sunde R [Ω]
			peak	converged	peak	converged	
1 - 1	L-type rod	1	106	99	98	83	82.4
1 - 2		2	44	42	40	35	49.3
2 - 1	rectangular plate	1	33	31	48	40	
2 - 2	width (w) 0.45 m	2	23	21	28	23	
3 - 1	rectangular plate	1	42	40	40	35	
3 - 2	width (w) 0.25 m	2	27	26	24	20	

(b) PG 2 - converged value at t = 450 ns

case	electrode shape	length x [m]	measured result				simulation [V/A]			Sunde R [Ω]
			steady state Rg	first peak		converged value [V/A]	first peak		converged value [V/A]	
				V [V] / I [A]	t[ns]		V [V] / I [A]	t [s]		
4 - 1	vertical pipe r = 25 mm	1	118	37 / 0.45	17	107.5	39.7 / 0.76	20	76.8	97.6
4 - 2		2	42	28 / 0.45	17	34.1	39.1 / 0.74	20	42.2	57.0
4 - 3		4	32	34 / 0.45	17	24.1	39.1 / 0.74	20	22.2	32.6
5 - 1	H-type rod Fig. 2 (d)	1	105	37 / 0.35	11	93.8	33.7 / 0.75	20	63.2	
5 - 2		2	40	43 / 0.45	14	34.1	33.6 / 0.75	20	35.3	
5 - 3		4	34	33 / 0.45	14	26.8	33.0 / 0.74	20	18.7	
6	4 plates / Fig. 2 (f)	4	36	31.5 / 0.35	11	30	35.2 / 0.74	20	19.3	
7	4 circular / Fig. 2 (g)	4	19	25 / 0.3	7	16.3	35.6 / 0.74	20	17.1	